Electronic Supplementary Material (ESI) for ChemComm.

Electronic Supporting Information (ESI)

Breathing-induced new phase transition in MIL-53(Al)-NH_2 metal-organic framework under high methane pressures

Linius Bolinois, Tanay Kundu, Xuerui Wang, Yuxiang Wang, Zhigang Hu, Kenny Koh and Dan Zhao*

Department of Chemical & Biomolecular Engineering, National University of Singapore, 4 Engineering Drive 4, 117585 Singapore

Correspondence and requests for materials should be addressed to D.Z. (E-mail: chezhao@nus.edu.sg)

Material synthesis

MIL-53(Al)

MIL-53(Al) was synthesized based on the procedure reported by T. Loiseau et. al.[1] Briefly, 3.83 g (10 mmol) of aluminum nitrate nonahydrate [$Al(NO_3)_3 \cdot 9H_2O$] was mixed with 0.830 g (5 mmol) of 1,4-benzenedicarboxylic acid (BDC) in 10 mL of water. The reagents were placed into a 23 mL teflon-lined autoclave and heated at 220 °C for 72 hours. The white powder was then washed with deonized water and dried overnight at 100 °C under vaccum. The product was then activated at 330 °C for 72 hours under vacuum to afford activated MIL-53(Al).

MIL-53(Al)-NH_2

MIL-53(Al)-NH_2 was synthesized based on the procedure reported by Tristan Lescouet et. al.[2] Briefly, 966 mg (4 mmol) of aluminum chloride hexahydrate ($AlCl_3 \cdot 6H_2O$) was mixed with 725 mg (4 mmol) of 2-aminoterephthalic acid (BDC-NH_2) in 15 mL of deonized water. The mixture was placed in a 23 mL teflon-lined autoclave and heated at 150 °C for 24 hours. The product was washed with water and N,N-dimethylformamide (DMF). In order to remove the BDC-NH_2 trapped in the pores of the solid, the powder was heated in 15 mL of DMF inside a 23 mL teflon-lined autoclave at 150 °C for 24 hours. The activation process was repeated twice (replacing the solvent with fresh DMF each time). The DMF was replaced by dichloromethane (DCM) by soaking for 3 days (changing a fresh set of DCM everyday). Lastly, the product was vacuumed overnight at 30 °C and finally heated at 200 °C for 10 hours to afford activated MIL-53(Al)-NH_2.

MIL-53(Al) with BDC/BDC-NH_2 mixed ligands

The synthesis of MIL-53(Al) with BDC/BDC-NH_2 mixed ligands were adapted from the procedure of the former group.[2] For a feeding containing x% of BDC-NH_2: 2.90 g (12 mmol) of $AlCl_3 \cdot 6H_2O$ was mixed with 2.174*x g (12*x mmol) of BDC-NH_2 and 1.994*(1-x) g (12*(1-x) mmol) of BDC in 50 mL of deonized water. The mixture was then placed into a 60 mL teflon-lined autoclave and heated at 150°C for 9 hours. The product was washed with water and DMF, then heated twice in 15mL of DMF, inside a 23 mL teflon-lined autoclave at 150 °C for 24 hours (replacing the solvent with fresh DMF each time). The product was then soaked in DCM for 3 days (changing a fresh set of DCM everyday). Finally, the product was vacuumed overnight at 30 °C, then heated at 250 °C for 10 hours.

HKUST-1

The synthesis of HKUST-1 (or CuBTC) was adapted from the report by Yaghi et al.[3] Briefly, 100 mg (0.51 mmol) of benzene-1,3,5-tricarboxylic acid (BTC) was mixed with 200 mg (0.82 mmol) of copper nitrate trihydrate in a mixture of 7 mL of DMF, 7 mL of ethanol and 7 mL of deionized water. The mixture was placed in a 60 mL teflon-lined autoclave and heated at 85 °C for 20 hours. The powder was then washed with DMF and soaked in DMF at 80°C for 24 hours. The sample was then soaked in methanol for 3 days, replacing the solvent every day. The solid was finally heated at 120 °C for 10 hours.

Characterization methods

PXRD measurement

The powder X-ray diffraction (PXRD) was performed using a Rigaku Miniflex 600 X-ray powder diffractometer. The simulated patterns of MIL-53(Al)-lt (CCDC 220477) and HKUST-1 (CCDC 112954) were used for comparison. For each experiment, approximately 50 mg of MOF powder was spread and pelletized on a glass sample holder. The operation was carried at room temperature (approximately 25°C) under normal atmospheric pressure, using Cu-K_α radiations at the speed of 1.5°/min and between 0 and 40°. For the MIL-53(Al) with BDC/BDC-NH_2 mixed ligands comparison, the same sample holder and sample amount was used for every measurement to limit the errors due to sample preparation and quantity.

The results are presented in **Fig. S2** and **S5**. Due to the different procedure of activation between MIL-53(Al)-NH_2 and MIL-53(Al) with BDC/BDC-NH_2 mixed ligands, we could not observe any trend in peak shift between the different samples.[4]

NMR measurement

^{1}H NMR spectrometry was performed using Spinsolve® benchtop NMR spectrometer. Prior to NMR tests, the MOF samples were digested in base solutions. Briefly, 10 mg of MOFs was dissolved in D_2O containing 0.4 mol/L of sodium hydroxide (NaOH), and the solution was placed into a sample tube. The magnetic field has a frequency of 42.5 MHz and we performed 90° pulses to get the Free Induction Decay (FID) signal. The FID signal was treated by MestreNova software to obtain the final spectrum.

The results are presented in **Fig. S3** and **Table S1.** The peak at 4.75 ppm is due to the presence of OH^- anions.

Nitrogen sorption at 77 K

The nitrogen sorption tests at 77 K from 0 to 1 bar were performed using Quantachrome AutoSorb iQ3 surface area and pore size analyzer. Typically, 50 mg of sample was used for each test. All the sample were activated at 150 °C for 10 hours. The temperature of the test was controlled by a liquid nitrogen bath. The results are presented in **Fig. S4** and **S6**.

The points taken for the calculation of BET surface area follow the rules of Rouquerol et al.[5] The BET surface area of MIL-53, MIL-53(Al)-NH_2 and MIL-53(Al) with BDC/BDC-NH_2 mixed ligands are presented in **Table S2** and are in the range of 900-1300 m^2/g. The BET surface area of HKUST-1 was calculated to be 1331 m^2/g and was obtained using a pore range of 0.004-0.02 P/P_0. The obtained surface areas agree with the literature.[3, 6]

The total CH_4 uptake of MIL-53(Al)-NH_2 has not been reported in the literature, possibly because of the lack of pore volume data of different phases. Using the N_2 adsorption data (**Fig. S4**), we calculated the pore volume of MIL-53(Al)-NH_2 for the *lp* phase and approximated this value for the *np* phase. For the *lp* phase, we chose the pressure point corresponding to the horizontal shape of the curve (avoiding the vertical increase near P/P_0 = 1.0). The pore volume of the *np* phase remains an approximation due the relatively low pressure of stability of this phase. The pore volume of MIL-53(Al) has been found to be 0.54 cm^3/g, which matches well with the literature data.[7] The results are shown in **Table S6.**

Characterization results

Characterization of MIL-53(Al) and MIL-53(Al)-NH_2

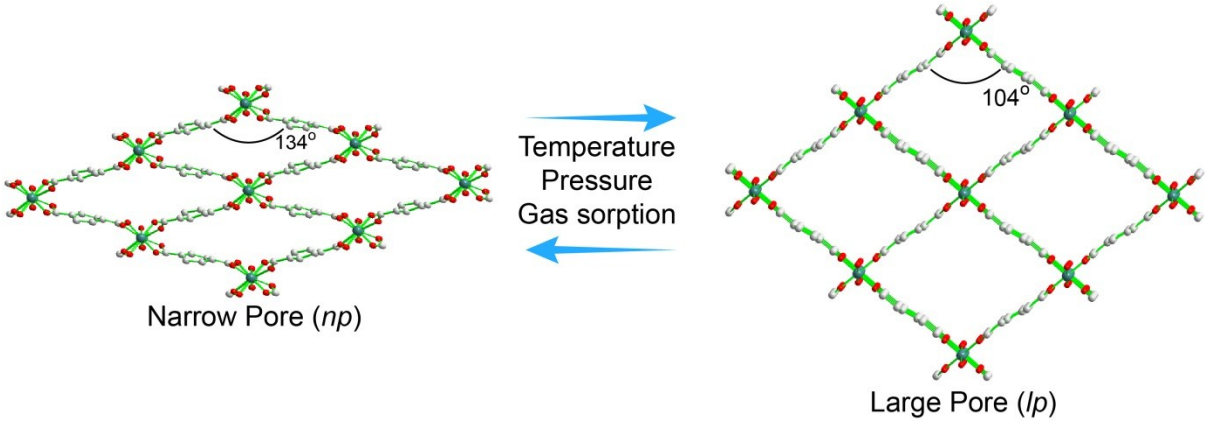

Figure S1. Structure of the narrow pore (*np*) and large pore (*lp*) phases of MIL-53(Al). The values of the angles data are obtained from the CCDC structures (220476 and 220477) reported by Ferey et al.[1]

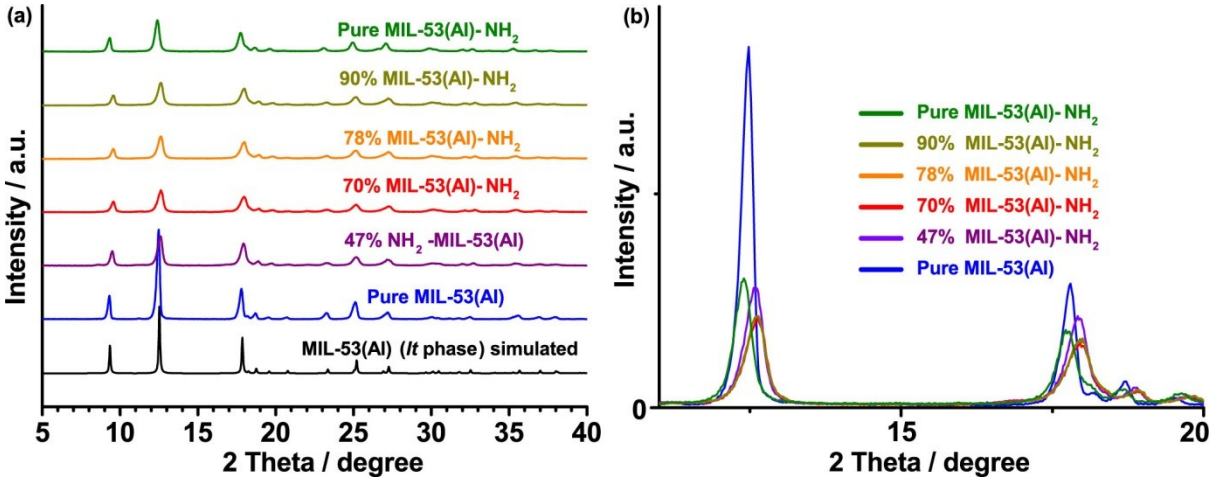

Figure S2. (a) PXRD of MIL-53(Al), MIL-53(Al)-NH_2 and MIL-53(Al) with BDC/BDC-NH_2 mixed ligands. (b) Zoom in view between 2θ = 11 and 20°.

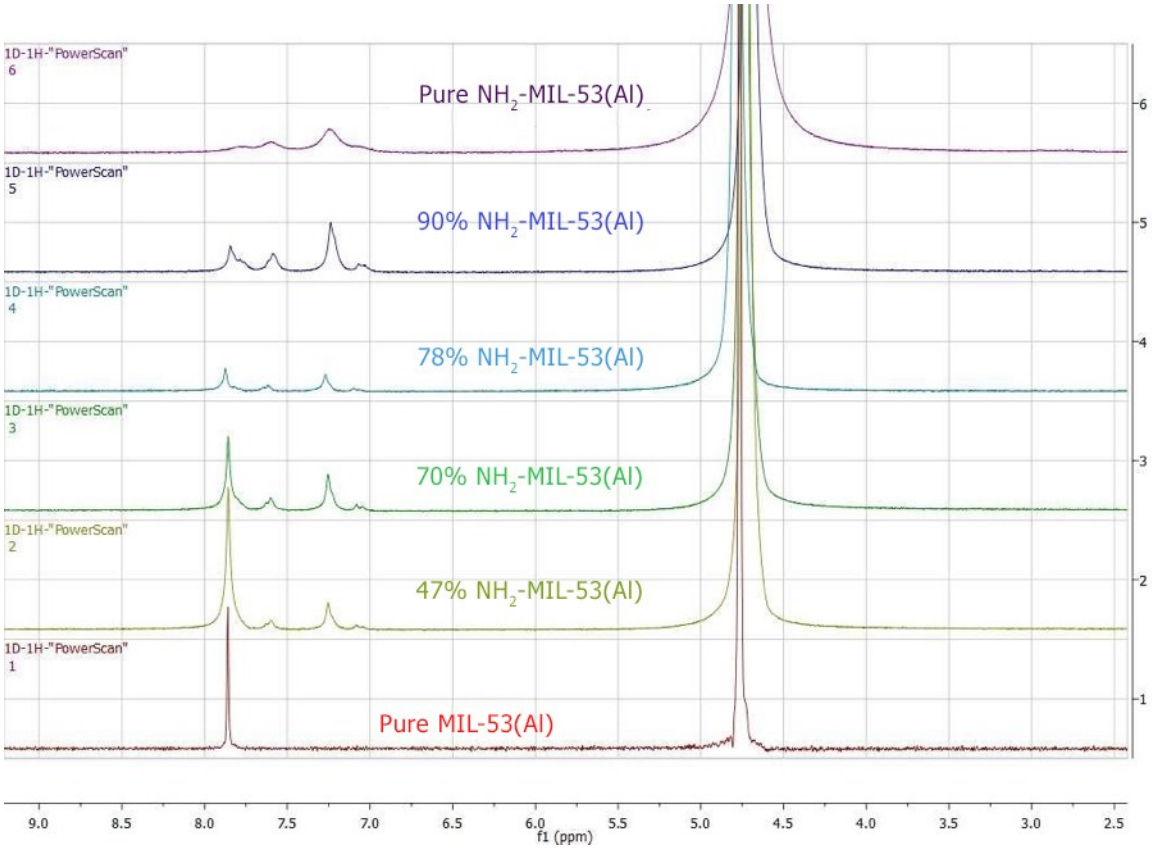

Figure S3. NMR of MIL-53(Al), MIL-53(Al)-NH_2 and MIL-53(Al) with BDC/BDC-NH_2 mixed ligands.

Table S1. Values of the concentration of MIL-53(Al)-NH_2 inside MIL-53(Al) synthesized with BDC/BDC-NH_2 mixed ligands.

Material	Feeding concentration	Estimated concentration from NMR
100% MIL-53(Al)-NH_2	100% BDC-NH_2/0%BDC	100% BDC-NH_2/0%BDC
90% MIL-53(Al)-NH_2	90% BDC-NH_2/10%BDC	90% BDC-NH_2/10%BDC
78% MIL-53(Al)-NH_2	67% BDC-NH_2/33%BDC	78% BDC-NH_2/22%BDC
70% MIL-53(Al)-NH_2	50% BDC-NH_2/50%BDC	70% BDC-NH_2/30%BDC
47% MIL-53(Al)-NH_2	20% BDC-NH_2/80%BDC	47% BDC-NH_2/53%BDC
Pure MIL-53(Al)	0% BDC-NH_2/100%BDC	0% BDC-NH_2/100%BDC

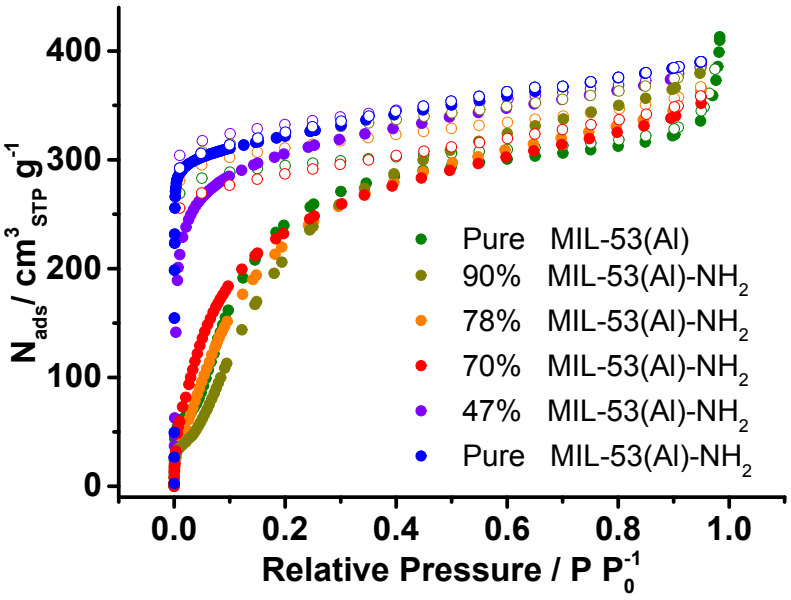

Figure S4. N_2 sorption isotherms at 77K of MIL-53(Al), MIL-53(Al)-NH_2 and MIL-53(Al) with BDC/BDC-NH_2 mixed ligands (closed, adsorption; open, desorption).

Table S2. BET surface areas calculated from N_2 adsorption isotherms of MIL-53(Al), MIL-53(Al)-NH_2 and MIL-53(Al) with BDC/BDC-NH_2 mixed ligands. The points taken for BET calculation follow the rules of Rouquerol et al.[5]

Material	Range of points taken for BET calculation	BET surface area
100% MIL-53(Al)-NH_2	0.12-0.26 P/P_0	947 m^2/g
90% MIL-53(Al)-NH_2	0.14-0.32 P/P_0	991 m^2/g
78% MIL-53(Al)-NH_2	0.1-0.34 P/P_0	909 m^2/g
70% MIL-53(Al)-NH_2	0.09-0.21 P/P_0	905 m^2/g
47% MIL-53(Al)-NH_2	0.06-0.1 P/P_0	1079 m^2/g
Pure MIL-53(Al)	0.005-0.03 P/P_0	1265 m^2/g

Characterisation of HKUST-1

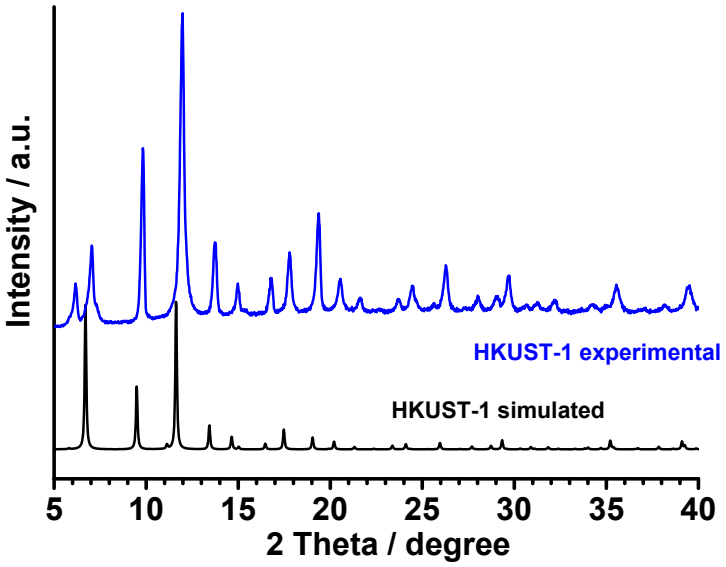

Figure S5. PXRD of HKUST-1 (experiment, blue; simulation, black).

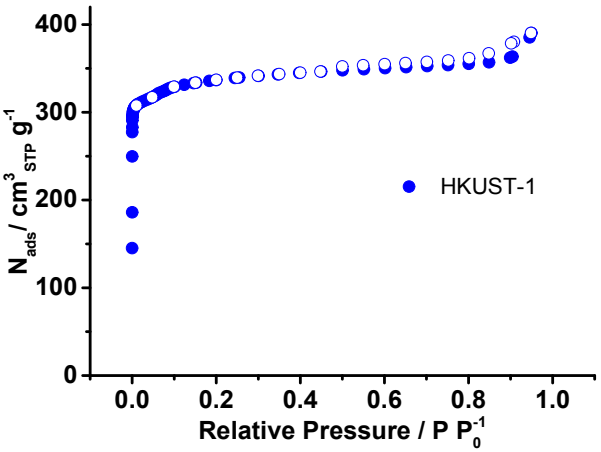

Figure S6. N_2 sorption isotherms at 77 K of HKUST-1 (closed, adsorption; open, desorption).

Equipment and method for high pressure methane sorption studies

Details of the high pressure methane sorption experiments

The high pressure methane sorption experiments were conducted using Quantachrome iSorbHP high pressure gas sorption system equipped with a gas booster and a cryocooler (**Fig. S7**). Methane cylinder was connected to a booster system in order to reach high pressures. The helium cylinder is used to calculate the void volume of the sample cell. Helmholtz equation of state was used for methane[8] and modified Benedict-Webb-Rubin/Jacobsen (mBWR-Jacobsen) equation of state was used for helium.[9]

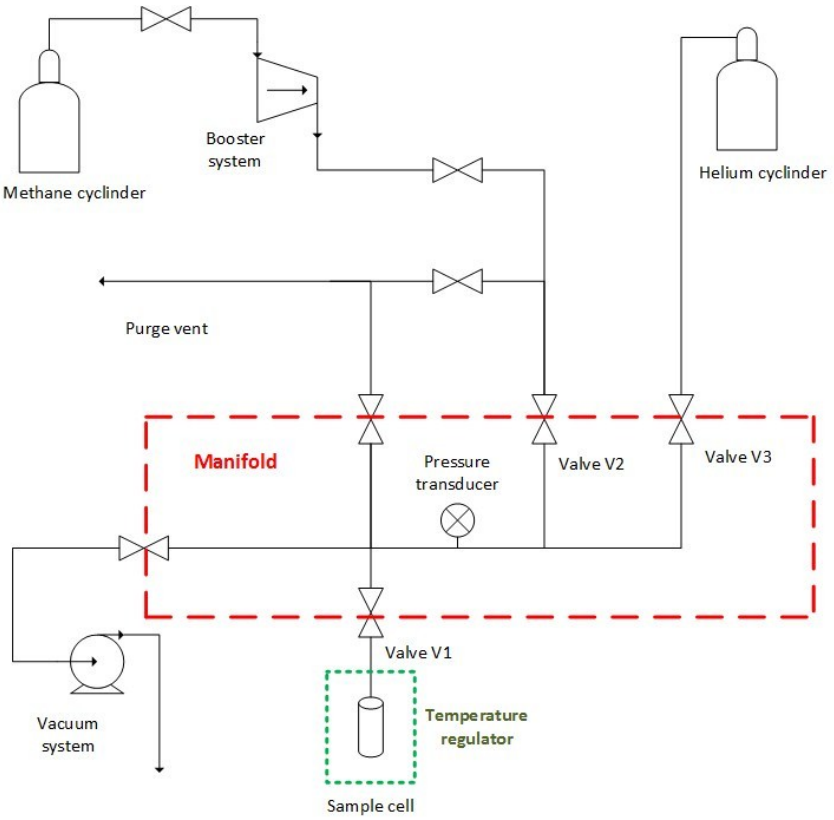

Figure S7. Simplified scheme of Quantachrome iSorbHP high pressure gas sorption system.

The working principle of this system is based on the difference of pressure before and after adsorption. In the beginning, the valve V1 is closed and the valve V2 is opened, which lets the adsorbate gas enter the manifold up to a pressure P_1. The amount of gas introduced in the system is given by:

$$n_1 = \frac{P_1 * V_M}{Z_M * R * T_M} \qquad \text{(Equation S1)}$$

Where V_M is the volume of the manifold (already known), T_M is the manifold temperature (normally 318 K), Z_M is the compressibility of the gas at the temperature T_M and the pressure P_1 (calculated from the gas law).

The valve V1 is then opened and the equilibrium pressure P_2 is recorded. There is no temperature equilibrium between the two compartments (manifold and sample cell) since they are maintained at

two different temperatures (318 K for the manifold and the analysis temperature for the sample cell). Therefore, a virtual temperature T_{eff} is used. The amount of gas in the total system is now:

$$n_2 = \frac{P_2 * (V_M + V_C)}{Z_{eff} * R * T_{eff}} \qquad \text{(Equation S2)}$$

Where V_C is the void volume of the sample cell (calculated below), T_{eff} is the effective temperature, Z_{eff} is the compressibility of the gas at the temperature T_{eff} and the pressure P_2 (calculated from the gas law).

The amount of gas adsorbed by the sample is then:

$$n_{excess} = n_1 - n_2 \qquad \text{(Equation S3)}$$

It is important to note that this amount always corresponds to the excess uptake, which is the supplementary amount of gas trapped in the adsorbed phase compared with the calculated density of the gas bulk phase at P and T.

Calibration

In order to perform the calculation mentioned above, the effective temperature T_{eff} and the void volume V_C of the system must be known. The latter are always changing, due to the sample cells used (which don't have the exact internal volume), the amount of sample introduced (which represents a certain volume) and the analysis temperature. Therefore, several tests need to be made using helium to determine these values.

The effective temperature is calculated by setting both the manifold and the sample cell at the temperature T_M, opening the valve V3 until a pressure P_1, opening the valve V1 and recording the pressure P_2, setting the sample cell at the analysis temperature T and recording the pressure P_3. If we assume that helium is not adsorbed by the sample, we can have the mass conservation:

$$\frac{P_2 * (V_M + V_C)}{Z_M * R * T_M} = \frac{P_3 * (V_M + V_C)}{Z_{eff} * R * T_{eff}} \qquad \text{(Equation S4)}$$

Which gives

$$T_{eff} * Z_{eff} = \frac{T_M * Z_M * P_3}{P_2} \qquad \text{(Equation S5)}$$

The unknown parameters in Equation S5 are T_{eff} and Z_{eff}, but the latter can be obtained with T_{eff} and state equation. Thus, it is possible to get T_{eff}.

The void volume is calculated after knowing T_{eff} by fixing the sample cell at the analysis temperature T, closing valve V1, opening valve V3 up to a pressure P_1, opening valve V1 and recording the pressure P_2. If we assume that helium is not adsorbed by the sample, we can have the mass conservation:

$$\frac{P_1 * V_M}{Z_M * R * T_M} = \frac{P_2 * (V_M + V_C)}{Z_{eff} * R * T_{eff}} \qquad \text{(Equation S6)}$$

Which gives

$$V_C = V_M * \left(\frac{P_1 * Z_{eff} * T_{eff}}{P_2 * Z_M * T_M} - 1\right) \qquad \text{(Equation S7)}$$

It is important to note that the two calculations are based on the assumption that helium is not adsorbed by the sample.

In volumetric experiments at high pressures, the temperature profile inside the cell changes with pressure, due to the heat capacity coefficients and heat transmission coefficients of the gas which are functions of the pressure. Hence, the calculation of the virtual temperature T_{eff} is not enough to get the final data and a subtraction of the raw data with blank has been found to be necessary, especially at high pressures and low temperatures.

Blank measurement

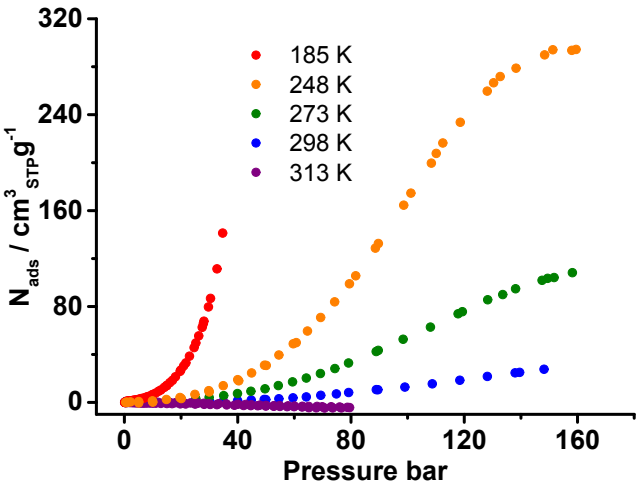

Figure S8. Blank curves for CH_4 adsorption. All the curves were measured using 0.5 mL (89 mg) of solid glass beads of 0.6-0.8 mm diameters.

As shown in **Fig. S8**, the higher the difference between the manifold temperature (308 K) and the analysis temperature, the more the deviation of CH_4 uptakes from 0 becomes prominent. For instance, the blank at 313 K shows a small uptake (order of 1 cm^3_{STP}/g) due to the small difference between the two temperatures (5 K). All the data presented in this study have been subtracted with the blank data collected at the corresponding temperatures, except for 313 K due to the very small amount detected.

Table S3. Void volume calculated for each test at high pressure (5 bar) for MIL-53(Al)-NH_2 and MIL-53(Al). All the blank curves were collected using 0.5 mL (89 mg) of solid glass beads of 0.6-0.8 nm diameters. The difference of void volume between the tests bellow and above 273 K is due to the change of temperature control system (tests bellow 273 K require a cooler which uses an extra tube).

Test	Void volume for the blank (0.5 mL glass beads)	Void volume for MIL-53(Al)-NH_2	Void volume for MIL-53(Al)
CH_4, 185 K, 35 bar	15.112 cm^3	15.350 cm^3	15.188 cm^3
CH_4, 248 K, 80 bar	14.572 cm^3	14.926 cm^3	14.624 cm^3
CH_4, 273 K, 80 bar	9.532 cm^3	9.779 cm^3	9.593 cm^3
CH_4, 298 K, 150 bar	9.392 cm^3	9.571 cm^3	9.358 cm^3
CH_4, 298 K, 120 bar	x	9.491 cm^3	x

CH_4, 298 K, 80 bar	x	9.521 cm^3	x
CH_4, 298 K, 50 bar	x	9.527 cm^3	x
CH_4, 313 K, 80 bar	9.245 cm^3	9.349 cm^3	x

Table S4. Void volume calculation results for mixed ligand variants of MIL-53(Al)-NH_2.

Mixture	Void volume for the test CH_4, 298 K, 80 bar
90% MIL-53(Al)-NH_2	9.331 cm^3
78% MIL-53(Al)-NH_2	9.268 cm^3
70% MIL-53(Al)-NH_2	9.448 cm^3
47% MIL-53(Al)-NH_2	9.376 cm^3

Table S5. Void volume calculation results for HKUST-1.

Test	Void volume for HKUST-1
CH_4, 298 K, 150 bar	9.512 cm^3
CH_4, 273 K, 150 bar	9.734 cm^3
CH_4, 248 K, 150 bar	14.737 cm^3

Definition of the Standard conditions of Temperature and Pressure (STP)

The notation STP refers to the equivalent volume of gas at a fixed condition of pressure and temperature which is stored inside the material. In our study, these conditions have been defined as P = 1.0 bar and T = 298 K (V_m = 24.0 L/mol).

For instance, 100 cm^3_{STP}/g means that one gram of material is able to store an amount of gas which would occupy 100 cm^3 if it were at 1.0 bar and 298 K.

Conversion from gravimetric uptake to uptake in molec. u.c.$^{-1}$

The following formula has been used for the conversion of gas uptakes:

$$Uptake\ in\ molec.\ u.c.^{-1} = Uptake\ in\ mol.\ g.^{-1} * M_{ads} \qquad \text{(Equation S8)}$$

Where M_{ads} is the molar mass of the adsorbent.

In this study, the calculated molar mass of MIL-53 is $M_{MIL\text{-}53}$ = 832 g mol^{-1}, considering the molecular formula [Al(OH)($C_8H_4O_4$)]. The molar mass of MIL-53-NH_2 is $M_{MIL\text{-}53\text{-}NH2}$ = 892 g mol^{-1}, considering the molecular formula of [Al(OH)($C_8H_5O_4N$)].

Validation using CH_4 uptakes of HKUST-1

In order to validate the equipment and method for high pressure gas sorption study, we performed high pressure CH_4 sorption studies using HKUST-1 (aka CuBTC),[7, 10]and compared the data with literature. We found an excess CH_4 uptake of 133 cm^3_{STP}/g at 298 K and 34.8 bar, which is close to what has been reported in the literature.[3, 6-7, 10]

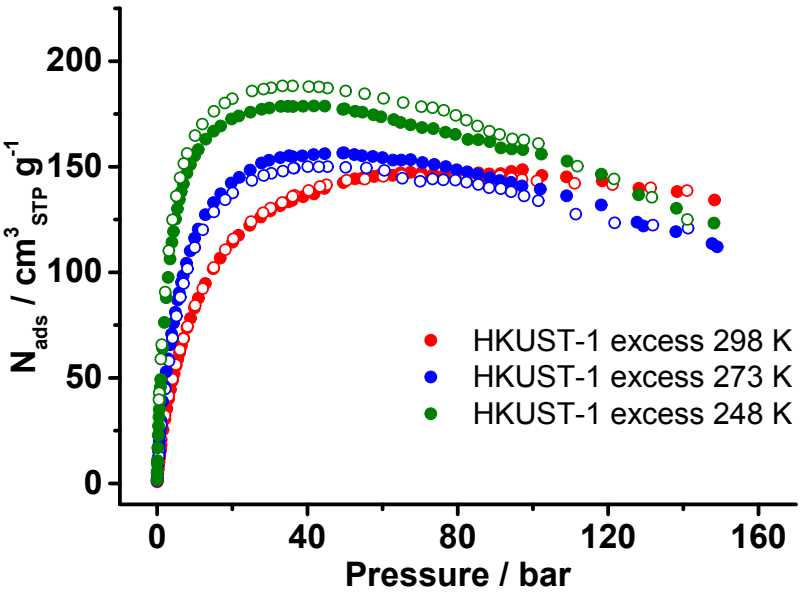

Figure S9. High pressure CH_4 uptakes in HKUST-1 measured by our high pressure gas sorption system with data calibration.

Explanation of the sorption curve tendency at high pressures

General definition of excess curves

The surface of the adsorbent generates attractive forces on the gas up to a distance corresponding to the Gibbs dividing surface. The region before this surface is called adsorbed region and has a specific density of the gas, and the region after the surface corresponds to the bulk gas. The sorption curves directly obtained from gas sorption experiments are always excess sorption, which is defined by the following equations:[7, 11]

$$n^e = n^{abs} - \rho^{bulk} * V^{ads} \quad \text{(Equation S9)}$$

$$n^e = \rho^{ads} * V^{ads} - \rho^{bulk} * V^{ads} \quad \text{(Equation S10)}$$

Where n^e is the excess uptake, n^{abs} is the absolute uptake, V^{ads} is the volume of the adsorbed region, ρ^{bulk} is the density of the bulk gas, ρ^{ads} is the density of the gas in the adsorbed region.

The absolute uptake corresponds to the amount of gas inside the adsorbed region. The excess uptake corresponds to the amount of gas which is added in the adsorbed region because of the presence of the adsorbent (i.e. the comparison with the amount of bulk phase gas which would have been in the same region in the absence of the absorbent).

Qualitative explanation of the drop in excess curves

At high pressures, the pores become saturated with gas while the bulk gas can still be compressed without condensation. Therefore, ρ^{ads} increases slower than ρ^{bulk}, which causes n^e to decrease.

Qualitative explanation of the increase of CH_4 uptake of MIL-53(Al)-NH_2 during desorption

MIL-53(Al)-NH_2 is in its *lp* phase at high pressures. During desorption, MIL-53(Al)-NH_2 initially stays in *lp* phase and the gas molecules remain trapped inside the pores. Therefore, ρ^{ads} remains relatively constant whereas ρ^{bulk} decreases, and this trend is more obvious in low pressures. This causes n^e to increase during the beginning of desorption processes. The same tendency can be observed in MIL-53(Al) (**Fig. S10**).

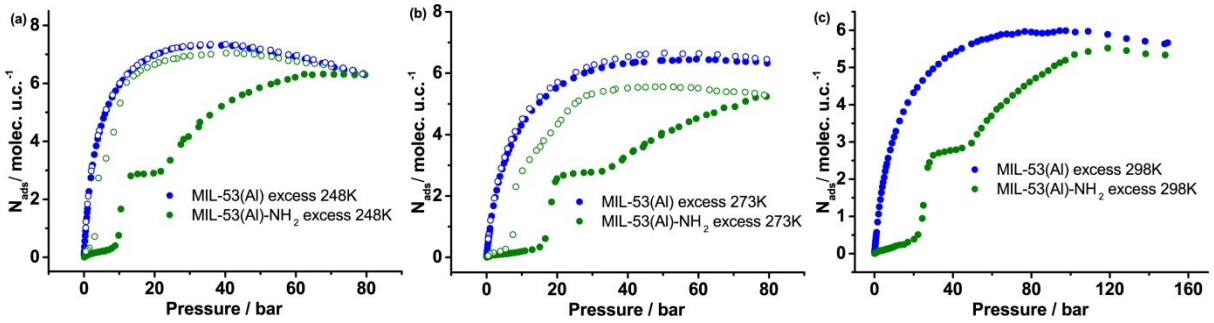

Figure S10. Excess CH_4 uptakes of MIL-53(Al) and MIL-53(Al)-NH_2 at 248 K (a), 273 K (b), and 298 K (c). Closed, adsorption; open, desorption.

Determination of the total CH_4 uptake

Pore volume determination

Up to our knowledge, the total CH_4 uptakes of MIL-53(Al)-NH_2 have not been reported in the literature, notably because of the lack of data concerning the total pore volume of this material under each phase. Using the N_2 adsorption data (**Fig. S4**), we calculated the pore volume of MIL-53(Al)-NH_2 for the *lp* phase and approximated this value for the *np* phase. For the *lp* phase, we chose the pressure point corresponding to the horizontal shape of the curve (avoiding the vertical increase near P/P_0 = 1.0). The pore volume of the *np* phase has been approximated due to the relatively low pressure of its stability domain. Accordingly, the pore volume of MIL-53(Al) has been calculated to be 0.54 cm^3/g, which matches well to the literature data.[7]

Table S6. Pore volume calculation of MIL-53(Al)-NH_2.

Phase	Pressure point taken	V_p value
vnp	x	0 cm^3/g (assumed)
np	0.024 P/P_0	0.10 cm^3/g
lp	0.90 P/P_0	0.50 cm^3/g

Determination of total gravimetric CH_4 uptake

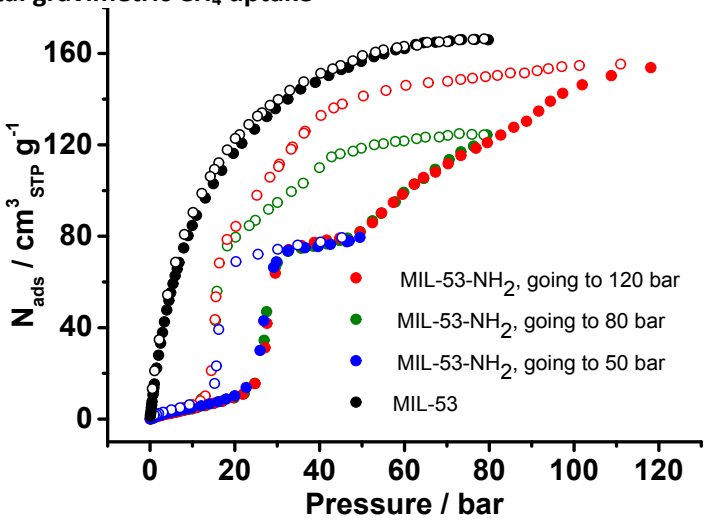

Figure S11. CH_4 excess uptakes of MIL-53(Al)-NH_2 under various pressures (closed, adsorption; open, desorption).

Fig. S11 shows that MIL-53(Al)-NH_2 exhibits phase changes at the same pressures regardless of the highest pressure point reached. For the plateau or Langmuir type-I shaped region of the curves, the pore volume was assumed to be constant to the one of the corresponding phase. The *np* to *lp* phase transition occurs during a large range of pressure, in which a linear changes of pore volume was assumed. The completion of the *lp* phase was assumed to occur at 120 bar at 298 K, which corresponds to the decrease of the excess uptake and the similarity between the adsorption of MIL-53(Al) and MIL-53(Al)-NH_2 (see **Fig. 2**). The total gravimetric CH_4 uptake was then calculated using the definition of the total uptake:

$$n^{tot} = n^e + \rho^{bulk}(P,T) * V_p \qquad \text{(Equation S11)}$$

Where n^{tot} is the total uptake, n^{e} is the excess uptake, V_p is the pore volume of the sample, ρ^{bulk} is the density of the bulk gas phase.

The values of ρ^{bulk} were found using Helmholtz equation of state.

Table S7. Determination of the pressure range of the phase stages and transitions in MIL-53(Al)-NH_2.

Phase stages and transitions	Pressure range
vnp phase	0-24 bar adsorption
vnp to *np* transition	24-32 bar adsorption
np phase	32-50 bar adsorption
np to *lp* phase	50-120 bar adsorption
lp phase	120-45 bar desorption
lp to *np* transition	45-18 bar desorption
np phase	Assumed not exist
np to *vnp* transition	18-10 bar desorption
vnp phase	10-0 bar desorption

Approximation of the volumetric CH_4 uptake

Material density is needed to convert the gravimetric CH_4 uptake data (obtained by experiments) into volumetric CH_4 uptake data:

$$n^{vol} = n^{grav} * \rho^{crystal} \quad \text{(Equation S12)}$$

Where n^{vol} is the uptake (total or excess) in volumetric unit ($cm^3_{gas\ at\ STP}/cm^3_{adsorbent}$ or v/v), n^{grav} is the uptake (total or excess) in gravimetric unit ($cm^3_{gas\ at\ STP}/g_{adsorbent}$), $\rho^{crystal}$ is the density of the crystal in g/cm^3.

Most MOFs are rigid, hence $\rho^{crystal}$ is assumed to be constant during the experiment and can be estimated by the value calculated from the perfect crystal structure. In the case of MIL-53(Al)-NH_2, the density is varying considerably with temperature and pressure due to phase transitions. The simulations obtained from Couck et al.[12] show a crystal unit cell volume of 927.4 $Å^3$ for the *vnp* phase under CH_4 pressure, 994.3 $Å^3$ for the *np* phase under CH_4 pressure and 1451.4 $Å^3$ for the *lp* phase under CO_2 pressure (the *lp* phase under CH_4 remains unstudied). This would correspond to a density of ρ = 1.60 g cm^{-3} for the *vnp* phase, ρ = 1.49 g cm^{-3} for the *np* phase and 1.02 g cm^{-3} for the *lp* phase.

In order to avoid the accumulation of errors, we decided to give an approximation of the deliverable capacity of the material in volumetric data. After going to 120 bar and returning at 65 bar, we assumed that the sample was completely in *lp* phase and that at 5.8 bar it was back to *vnp* phase. Therefore, the deliverable capacity was calculated as:

$$deliverable\ capacity = uptake\ at\ 65\ bar\ (in\ cm^3/g)\ * \rho^{lp} - \ uptake\ at\ 5.8\ bar\ (in\ cm^3/g)\ * \rho^{vnp} \quad \text{(Equation S13)}$$

Definition of the deliverable capacity

The deliverable capacity corresponds to the amount of gas which can be stored and released during the working cycles. In a classic cycle, adsorption corresponds to the gas storage process whereas desorption corresponds to the delivery process. Therefore, the deliverable capacity is defined as the difference of uptakes between the adsorption pressure and the desorption pressure. Due to the working range of compressors used for on-board natural gas storage, the adsorption pressure is conventionally fixed at 35 or 65 bar, whereas the desorption pressure is fixed near 5 bar (5.8 bar in the most recent studies).[7, 13]

In this study, we found that due to the hysteresis effect of MIL-53(Al)-NH_2, the CH_4 uptake at 65 bar could be much higher if the sample was previously pressurized at 120 bar. Thus, we can imagine a new kind of definition of the deliverable capacity, which would be the difference between the uptake at 65 bar during desorption (after being pressurized at high pressures) and the uptake at 5.8 bar during desorption. This new process can only be interesting for breathing MOFs with hysteresis at high pressures. Indeed, for typical Langmuir type-I isotherms, the values for adsorption and desorption are the same whatever the pressurization history of the sample.

Another way to use the hysteresis effect is to use the stability of the *lp* phase. As expressed in the main article, once the *lp* phase is triggered, it will remain stable unless the pressure is reduced bellow 45 bar at 298 K. We also found that there could be other methods to trigger the *lp* phase, such as cycling with pressure. Therefore, the deliverable capacity could be defined as the difference between the uptake at 65 bar and 298 K (whatever the pressure/temperature pathway taken) and the uptake at 5.8 bar and 298 K.

The schematic representations of the deliverable capacities are shown in **Fig. S12**.

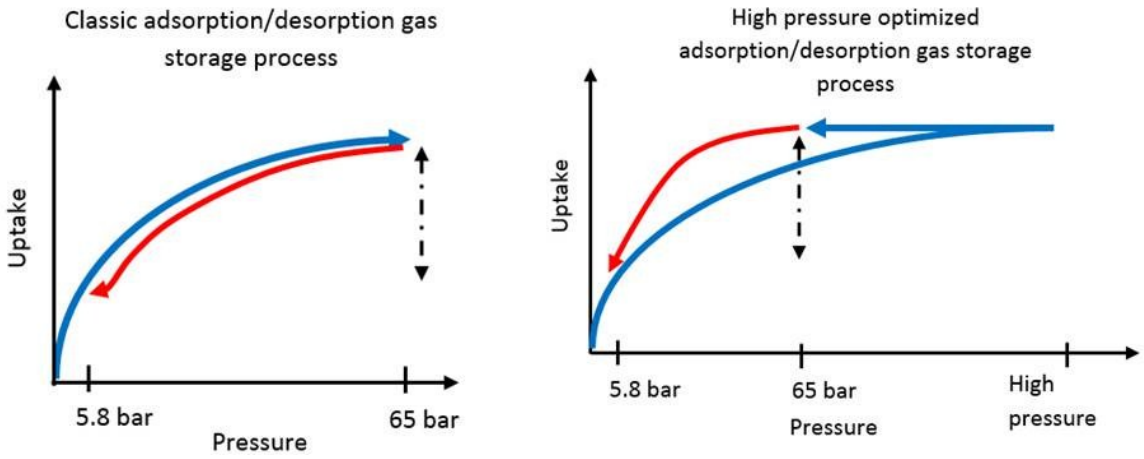

Figure S12. Schematic representation of the classic adsorption/desorption gas storage process compared with our proposition of high pressure adsorption/desorption process. The blue curve represents the storage stage whereas the red curve represents the delivery stage.

Based on the above discussion, we calculated the deliverable capacities of the MOFs in this study (**Table S8**). The deliverable capacity was defined using the uptake at 65 bar during desorption (after being pressurized to 80 bar) and the uptake at 5.8 bar during desorption. For all the calculations, the exact uptakes at 65.0, 35.0 and 5.8 bar have been calculated using a linear regression between the closest experimental pressure points from these values. Note that the values are excess values. Indeed, it was challenging to calculate the total uptake of MIL-53(Al) with BDC/BDC-NH_2 mixed ligands due to the variation of the pore volume.

Table S8. Approximation of the deliverable capacity of MIL-53(Al), MIL-53(Al)-NH_2 and MIL-53(Al) with BDC/BDC-NH_2 mixed ligands.

Material	CH_4 uptake at 65 bar during desorption (after being pressurized to 80 bar)	CH_4 uptake at 5.8 bar during desorption (after being pressurized to 80 bar)	Approximation of the deliverable capacity
100% MIL-53(Al)-NH_2	123 cm^3/g	4 cm^3/g	119 cm^3/g
90% MIL-53(Al)-NH_2	128 cm^3/g	7 cm^3/g	121 cm^3/g
78% MIL-53(Al)-NH_2	139 cm^3/g	15 cm^3/g	124 cm^3/g
70% MIL-53(Al)-NH_2	142 cm^3/g	29 cm^3/g	113 cm^3/g
47% MIL-53(Al)-NH_2	149 cm^3/g	53 cm^3/g	96 cm^3/g
Pure MIL-53(Al)	165 cm^3/g	67 cm^3/g	98 cm^3/g

Nitrogen scanning

In order to validate the results in **Fig. 5**, we chose to compare the behaviors of MIL-53(Al) and HKUST-1, which can be assumed to be rigid at the testing conditions. The results are shown in **Fig. S13**. The high increase of 22 cc/g in MIL-53(Al)-NH_2 compared to minute increase (~4cc/g) observed in HKUST-1 and MIL-53(Al) indicate the potential of flexibile MOFs in accommodating large amounts of gas molecules at low pressures upon multiple adsorption-desorption cycles, which is missing in rigid MOFs.

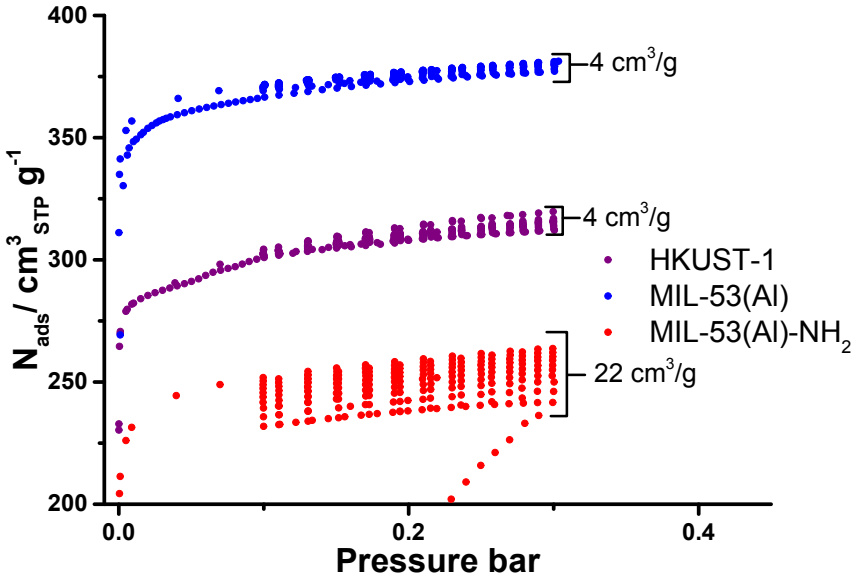

Figure S13. Comparison between HKUST-1, MIL-53(Al) and MIL-53(Al)-NH_2 over the same cycle (10 adsorption-desorption cycles of N_2 at 77 K between 0.1 and 0.3 bar followed by desorption).

References

1. T. Loiseau, C. Serre, C. Huguenard, G. Fink, F. Taulelle, M. Henry, T. Bataille and G. Férey, *Chem.-Eur. J.*, 2004, **10**, 1373.
2. T. Lescouet, E. Kockrick, G. Bergeret, M. Pera-Titus, S. Aguado and D. Farrusseng, *J. Mater. Chem.*, 2012, **22**, 10287.
3. J. L. C. Rowsell and O. M. Yaghi, *J. Am. Chem. Soc.*, 2006, **128**, 1304.
4. S. Marx, W. Kleist, J. Huang, M. Maciejewski and A. Baiker, *Dalton Trans.*, 2010, **39**, 3795.
5. J. Rouquerol, P. Llewellyn and F. Rouquerol, in *Characterization of Porous Solids Vii - Proceedings of the 7th International Symposium on the Characterization of Porous Solids*, eds. P. L. Llewellyn, F. Rodriquez Reinoso, J. Rouqerol and N. Seaton, Elsevier Science Bv, Amsterdam, 2006, vol. 160, pp. 49.
6. (a) M. Pera-Titus, T. Lescouet, S. Aguado and D. Farrusseng, *J. Phys. Chem. C*, 2012, **116**, 9507; (b) P. Rallapalli, D. Patil, K. P. Prasanth, R. S. Somani, R. V. Jasra and H. C. Bajaj, *J. Porous Mat.*, 2010, **17**, 523.
7. J. A. Mason, M. Veenstra and J. R. Long, *Chem. Sci.*, 2014, **5**, 32.
8. U. Setzmann and W. Wagner, *J. Phys. Chem. Ref. Data*, 1991, **20**, 1061.
9. R. D. A. McCarty, V.D., *Adv. Cryo. Eng.*, 1990, **35**, 1465.
10. S. S. Y. Chui, S. M. F. Lo, J. P. H. Charmant, A. G. Orpen and I. D. Williams, *Science*, 1999, **283**, 1148.
11. A. L. Myers and P. A. Monson, *Langmuir*, 2002, **18**, 10261.
12. S. Couck, E. Gobechiya, C. E. A. Kirschhock, P. Serra-Crespo, J. Juan-Alcaniz, A. M. Joaristi, E. Stavitski, J. Gascon, F. Kapteijn, G. V. Baron and J. F. M. Denayer, *ChemSusChem*, 2012, **5**, 740.
13. (a) J. A. Mason, J. Oktawiec, M. K. Taylor, M. R. Hudson, J. Rodriguez, J. E. Bachman, M. I. Gonzalez, A. Cervellino, A. Guagliardi, C. M. Brown, P. L. Llewellyn, N. Masciocchi and J. R. Long, *Nature*, 2015, **527**, 357; (b) C. M. Simon, J. Kim, D. A. Gomez-Gualdron, J. S. Camp, Y. G. Chung, R. L. Martin, R. Mercado, M. W. Deem, D. Gunter, M. Haranczyk, D. S. Sholl, R. Q. Snurr and B. Smit, *Energy Environ. Sci.*, 2015, **8**, 1190.